Human Molecular Genetics, 2007, Vol. 16, No. 17 **2031–2039**
doi:10.1093/hmg/ddm151
Advance Access published on June 20, 2007

Mechanistic insight into the dominant mode of the Parkinson's disease-associated G2019S LRRK2 mutation

Berta Luzón-Toro[1], Elena Rubio de la Torre[1], Asunción Delgado[1], Jordi Pérez-Tur[2] and Sabine Hilfiker[1,*]

[1]Institute of Parasitology and Biomedicine 'López-Neyra', Spanish National Research Council (CSIC), 18100 Granada, Spain and [2]Institute of Biomedicine, Spanish National Research Council (CSIC), 46010 Valencia, Spain

Received April 30, 2007; Revised and Accepted June 14, 2007

Pathogenic mutations in the leucine-rich repeat kinase-2 (*LRRK2*) gene cause autosomal-dominant and certain cases of sporadic Parkinson's disease (PD). The G2019S substitution in LRRK2 is the most common genetic determinant of PD identified so far, and maps to a specific region of the kinase domain called the activation segment. Here, we show that autophosphorylation of LRRK2 is an intermolecular reaction and targets two residues within the activation segment. The prominent pathogenic G2019S mutation in LRRK2 results in altered autophosphorylation, and increased autophosphorylation and substrate phosphorylation, through a process that seems to involve reorganization of the activation segment. Our results suggest a molecular mechanistic explanation for how the G2019S mutation enhances the catalytic activity of LRRK2, thereby leading to pathogenicity. These findings have important implications for therapeutic strategies in PD.

INTRODUCTION

Dominant mutations in the leucine-rich repeat kinase-2 (*LRRK2*) gene are associated with both familial and sporadic Parkinson's disease (PD) (1,2). One specific missense mutation in *LRRK2* (G2019S) comprises the most common genetic determinant of PD to date. While initially reported with a frequency of 5–6% for familial and 1–2% for sporadic PD cases (3–7), subsequent studies have revealed that mutation frequency is dependent on ethnicity (8–11). Extremely high frequency for the G2019S mutation has been reported in Ashkenazi Jews (overall around 14%) and North African Berber-Arabs (around 30%) (8,9), but low frequency in Chinese (10,11). In addition, the majority of G2019S carriers share a common haplotype dating several thousand years back (12,13). Even though the reported high frequency indicates a crucial role for mutant LRRK2 in PD susceptibility, incomplete penetrance (2,12,14–16) suggests that additional environmental and/or epigenetic factors may regulate the expression of the PD phenotype.

The *LRRK2* gene encodes for a large protein kinase (280 kDa) with multiple domains (17). These include different repeat sequences at the N-terminus such as ankyrin and leucine-rich repeats (LRR), a Roc GTPase domain, followed by a C-terminal of Roc (COR) domain, a kinase domain and WD40 repeats (18,19). While the presence of multiple protein–protein interaction domains hints towards a scaffolding function, the presence of GTPase and kinase domains suggests that LRRK2 may perform catalytic role(s). Indeed, biochemical efforts to characterize LRRK2 have revealed that it harbors kinase activity *in vitro*, which seems to be regulated by its GTP binding and/or GTPase activity (20,21), such that multiple signal transduction cascades may impact upon LRRK2 function.

The prevalent G2019S mutation lies within the activation segment of the kinase domain of LRRK2. Interestingly, the activity of a large variety of protein kinases is controlled by activation segment conformation, whereby phosphorylation of this segment leads to a conformational change switching the kinase from an 'off'- to an 'on'-state (22). Thus, the position of the G2019S mutation within the primary sequence suggests that it may directly modulate the catalytic status of LRRK2. This possibility has been addressed by overexpressing wild-type and mutant LRRK2 in tissue culture cells,

*To whom correspondence should be addressed at: Parque Tecnológico de Ciencias de la Salud, Avda del Conocimiento s/n, 18100 Granada, Spain. Tel: +34 958181654; Fax: +34 958181632; Email: sabine.hilfiker@ipb.csic.es

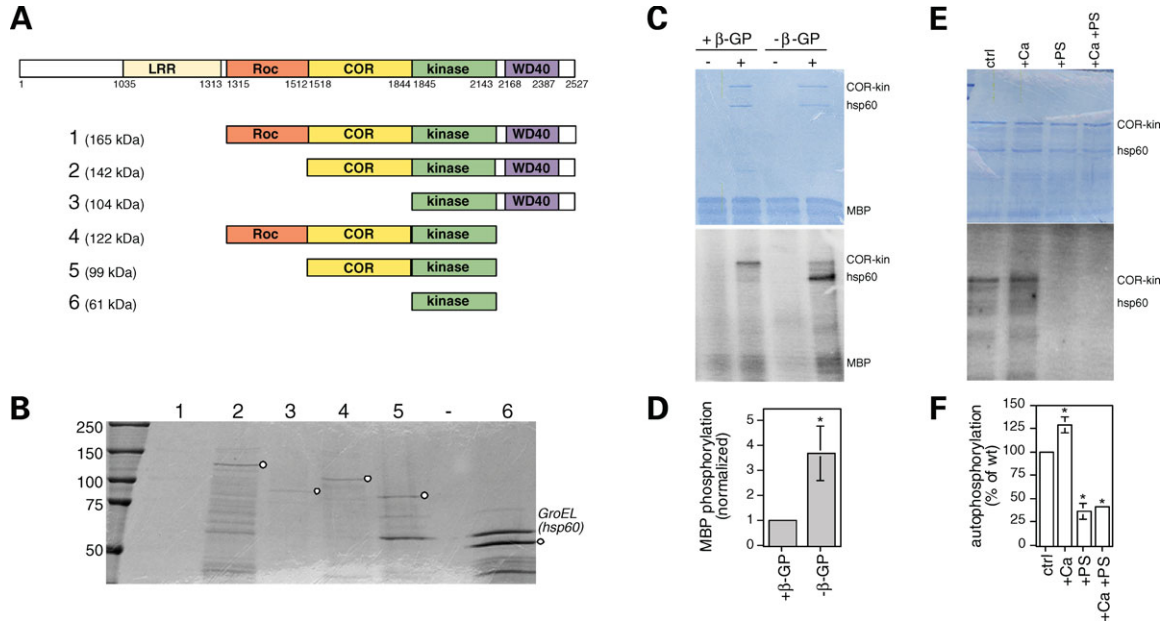

Figure 1. Characterization of the catalytic activity of recombinant LRRK2. (**A**) Schematic representation of LRRK2 domain structure, with domain boundaries shown by amino acid residue numbers beneath, and of recombinant LRRK2 domain combinations (constructs 1–6) analysed in the present study. The predicted molecular mass of each construct (including the GST moiety) is indicated in brackets. (**B**) The different recombinant GST-LRRK2 domains were purified as described in Materials and Methods, and analysed for purity by SDS–PAGE and Coomassie staining. While the largest fusion protein (construct 1) was entirely insoluble, other domain combinations (constructs 2–6) could be purified in soluble form (open circles). Significant amounts of GroEL (bacterial hsp60, as determined by mass spectroscopy) co-purified with all constructs containing the kinase domain. Positions of molecular weight markers are shown on the left (in kDa). (**C**) Autophosphorylation and model substrate phosphorylation of 1 μg of purified recombinant LRRK2 domain (COR-kinase) (COR-kin) and 10 μg of MBP. Top: Coomassie; Bottom: ^{32}P autoradiograph. Phosphorylation reactions were performed in the presence or absence of 10 mM β-glycerolphosphate (±β-GP), respectively. Note that the presence of β-glycerolphosphate preferentially stimulated autophosphorylation over substrate phosphorylation. (**D**) Quantitation of MBP phosphorylation assays of the type depicted in (C) (mean ± SEM; $n = 4$). (**E**) Autophosphorylation of 1 μg of purified recombinant LRRK2 domain (COR-kinase) in the presence or absence of 1 mM $CaCl_2$ or 50 μg/ml phosphatidylserine (PS). Top: Coomassie; Bottom: ^{32}P autoradiograph. (**F**) Quantitation of assays of the type depicted in (E) (mean ± SEM; $n = 4$). Samples were subjected to autophosphorylation reactions in phosphorylation buffer (50 mM HEPES pH 7.4, 5 mM $MgCl_2$, 5 mM $MnCl_2$, 0.5 mM DTT) for 30 min at 24°C. Reactions were stopped with sample buffer and boiling for 5 min, followed by SDS–PAGE and staining with Coomassie blue dye. Radioactive bands were quantified using ImageQuant (Molecular Dynamics) and corrected for background values. Differences in protein amounts were quantified on Coomassie stained gels using QuantityOne (Bio-Rad), and corrected for background values. Radioactivity values were corrected for differences in protein loading. Error bars represent SEM. *, $P < 0.05$.

followed by measurements of catalytic activity of immunoprecipitated protein. Indeed, the G2019S mutation was found to increase the kinase activity of LRRK2 (23–25), in line with an expected gain-of-function mechanism for its dominant transmission. Furthermore, increased kinase activity of G2019S-mutant LRRK2 resulted in increased apparent neurotoxicity (23–25). Although these studies suggest that enhanced kinase activity may underlie the mechanism of PD in G2019S carriers, the precise molecular basis by which this mutation enhances LRRK2 catalytic activity remains to be established.

In the present study, we have examined the effect of the G2019S mutation on the catalytic activity of the purified, recombinant LRRK2 kinase domain *in vitro*. For this purpose, we established conditions to purify recombinant kinase *in vitro* in its catalytically active form, and determined optimal buffer conditions for autophosphorylation and model substrate phosphorylation assays. We demonstrate that catalytic activity of recombinant LRRK2 kinase is regulated by intermolecular autophosphorylation at two residues within the activation segment. In addition, we find that the mutation generates a novel phosphorylation site within the activation segment. By mutating select other residues within the activation segment of wild-type and mutant kinase domain, we find that the increased catalytic activity of the G2019S mutant seems to involve reorganization of this segment to mimick the active state of the kinase. Together, our results suggest a molecular mechanism by which the G2019S mutation enhances the catalytic activity of LRRK2, which has important implications for the screening and design of kinase inhibitors as possible treatment option for PD.

RESULTS

Catalytic activity of recombinant LRRK2 kinase

To establish *in vitro* phosphorylation reactions using purified, recombinant LRRK2, we generated a series of GST-fusion protein constructs encoding for various domains (Fig. 1A). While the largest LRRK2 protein containing the Roc, COR, kinase and WD40 domains was entirely insoluble under our purification conditions, shorter domain combinations yielded soluble proteins (Fig. 1B). The GST moiety enhanced solubility, which greatly decreased when GST-fusion proteins were cleaved by thrombin to release the GST tag (data not shown). A prominent contaminant, identified as hsp60 by mass

spectroscopy, copurified with all fusion proteins (Fig. 1B). This contaminant copurified with fusion proteins containing the kinase domain either on its own or in combination (Fig. 1B), but not with recombinant proteins devoid of kinase domain (data not shown). These data indicate that hsp60 may perform a chaperone action in maintaining the proper folding of recombinant LRRK2 kinase domain in *Escherichia coli*, similar to that suggested for the reported hsp90 interaction with full-length LRRK2 in mammalian cells (26). Since reasonably large amounts of purified proteins could only be obtained with COR-kinase and kinase constructs, subsequent studies were performed with those GST-tagged LRRK2 proteins only.

To characterize the catalytic activity of recombinant LRRK2, the purified COR-kinase and kinase domains were subjected to autophosphorylation and model substrate phosphorylation assays *in vitro*. Recombinant LRRK2 kinase was capable of autophosphorylation and substrate phosphorylation using myelin basic protein (MBP) as a model substrate (Fig. 1C and D). While recombinant GST was not phosphorylated (data not shown), the copurifying hsp60 protein served as an additional model substrate for recombinant LRRK2 kinase activity (Fig. 1C). Using a variety of buffer conditions, catalytic activity was found to be dependent on the presence of Mn^{2+}, in contrast to previous reports using overexpressed full-length LRRK2 immunoprecipitated from mammalian cells (20,23,24,26). This dependency could not be overcome by increasing the concentration of Mg^{2+}, suggesting that recombinant LRRK2 kinase is an Mn^{2+}-preferring kinase *in vitro* (data not shown). The presence of β-glycerolphosphate favored autophosphorylation over substrate phosphorylation (Fig. 1C and D). Catalytic activity was thermolabile, such that all reactions had to be performed at 24°C, and enzyme activity was found to be slightly enhanced by Ca^{2+} and profoundly inhibited by phospholipids (Fig. 1E and F). Together, these results establish the conditions necessary to measure the catalytic activity of recombinant LRRK2 kinase, which should aid in future studies aimed at screening LRRK2 kinase inhibitors *in vitro*.

To assure that the observed autophosphorylation and substrate phosphorylation were due to the catalytic activity of recombinant LRRK2, rather than the presence of a bacterial co-purifying kinase, we analyzed constructs predicted to decrease the kinase activity of LRRK2. For this purpose, we generated mutant D2017A, which alters the Mg^{2+} binding loop, R1993A, a residue in the catalytic loop and K1906M, which abolishes ATP binding (22,27). Both D2017A ($54 \pm 7\%$; mean $\pm$ SEM; $n = 4$) and R1993A ($31 \pm 11\%$; mean $\pm$ SEM; $n = 4$) mutations decreased, whereas the K1906M mutation abolished autophosphorylation (Fig. 2A and B), indicating that we are measuring inherent catalytic activity of LRRK2. In addition, the ability of LRRK2 to phosphorylate both itself as well as a model substrate (Fig. 1C and D) suggests that basal LRRK2 activity *in vitro* is independent of an activating kinase.

Intermolecular nature and sites of autophosphorylation

Autophosphorylation of a kinase can represent either a true intramolecular event, or transphosphorylation of one kinase molecule by another. To distinguish between the two processes, we performed kinase reactions using two electrophoretically distinct forms of LRRK2, one of which was catalytically competent (kinase domain only) and the other inactive (mutant COR-kinase domain) (Fig. 2C). In such mixed kinase reactions, the active kinase was able to phosphorylate a kinase-dead mutant (COR-kinase-K1906M mutant), indicating that autophosphorylation is an intermolecular reaction (Fig. 2D and E).

Next, we aimed to determine the autophosphorylation sites within recombinant LRRK2 kinase. The most common regulatory mechanism for kinase activity involves activation loop phosphorylation (22). In protein kinases whose crystal structures have been determined in both inactive and active forms, the non-phosphorylated activation loop usually binds to another region of the kinase domain, trapping it in an inactive conformation. Kinase activation is triggered by a critical change in the conformation of the activation loop, mostly induced by either autophosphorylation or exogenous phosphorylation by upstream activating kinases (22). LRRK2 kinase contains three putative residues (T2031, S2032 and T2035) within the activation loop which could serve as autophosphorylation sites (Fig. 3A). To determine whether autophosphorylation targets those residues, we constructed proteins with mutations of the Ser or Thr residue within the activation loop and determined their effects on LRRK2 autophosphorylation and activity. While single mutations of T2031A or S2032A caused a significant reduction in LRRK2 activity, these mutants did retain some basal activity (Fig. 3B and C). In contrast, when the two residues were simultaneously mutated to Ala (T2031A/S2032A), the activity of this mutant was almost completely lost (Fig. 3B and C), comparable to that of the kinase-dead mutant (Fig. 2A and B). Similarly, the T2035A mutant did not show detectable autophosphorylation (Fig. 3B and C). In transphosphorylation assays, the T2035A mutant incorporated phosphate comparable to wild-type, but almost no phosphate incorporation was detectable in the T2031A/S2032A double mutant LRRK2 (Fig. 3D and E). Together, these data establish T2031 and S2032 as the key regulatory phosphorylation sites required for LRRK2 activation, and indicate that T2035 is important for catalytic activity, but does not serve as a phosphate acceptor.

Mechanistic underpinnings of G2019S mutation

The activation loop is anchored into the kinase structure at its N-terminus by a conserved DYG sequence (Fig. 3A). This sequence is part of the Mg^{2+}-binding loop and is altered by the prominent G2019S mutation. The G2019S mutant presumably did not prevent Mg^{2+} binding, as it showed autophosphorylation *in vitro*. On the contrary, G2019S mutant LRRK2 kinase displayed around 3-fold higher autophosphorylation activity as compared to wild-type kinase (Fig. 4A). In contrast, the pathogenic I2020T mutation adjacent to G2019 within the N-terminal hinge region of the loop did not significantly affect activity. Similarly, a putatively pathogenic mutation in the kinase domain (R1941H) and a pathogenic mutation in the COR domain (Y1699C) were without effect (Fig. 4A). Intriguingly, the pathogenic I2012T mutation,

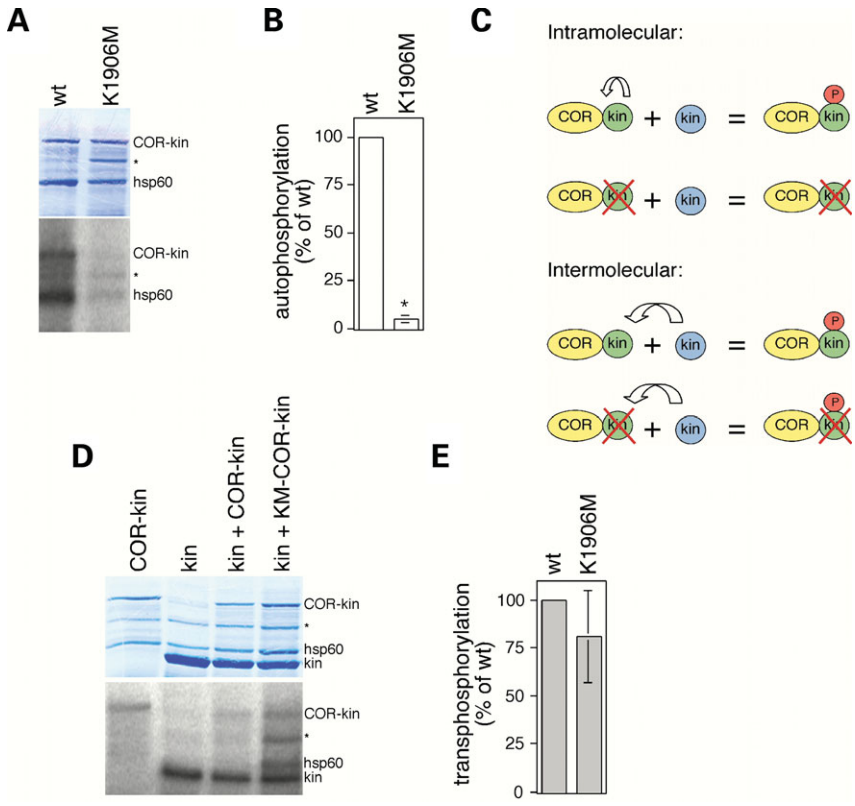

Figure 2. Intermolecular nature of autophosphorylation of recombinant LRRK2 kinase. (**A**) Autophosphorylation of wild-type or catalytically impaired COR-kinase (COR-kin) mutant. Top: Coomassie; Bottom: ^{32}P autoradiograph. Experiments and data analysis were performed as described in legend to Figure 1. *, contaminant observed in some protein preparations. (**B**) Quantitation of experiments of the type depicted in (A). The extent of autophosphorylation was compared to results with wild-type protein and charted as percent of the control measurement. Average values from eight independent experiments are shown. (**C**) Schematic diagram depicting the distinct outcomes of a transphosphorylation experiment. If autophosphorylation is an intramolecular reaction, mutant, catalytically inactive COR-kinase is not phosphorylated. If autophosphorylation is an intermolecular reaction, mutant COR-kinase can be phosphorylated by active kinase molecules in the reaction mixture, leading to phosphate incorporation. (**D**) Example of a transphosphorylation experiment using wild-type (COR-kin) or the K1906M point-mutant COR-kinase protein (KM-COR-kin), together with wild-type kinase domain protein (kin). Top: Coomassie; Bottom: ^{32}P autoradiograph. *, contaminant observed in some protein preparations. (**E**) Quantitation of experiments of the type depicted in (D). Experiments and data analysis were performed as described in legend to Figure 1. The extent of phosphate incorporation was compared to results with wild-type protein and charted as percent of the control measurement. Average values from four independent experiments are shown. Error bars represent SEM. *, $P < 0.05$.

situated within the Mg^{2+} binding loop (Fig. 3A), displayed a small but significant decrease in catalytic activity (Fig. 4A). Thus, of all the mutations analyzed in this study, only G2019S enhanced LRRK2 catalytic activity. The enhanced autophosphorylation of the G2019S mutation was paralleled by enhanced substrate phosphorylation (Fig. 4B). These data indicate that the G2019S mutation results in a direct increase in catalytic activity of recombinant LRRK2, as previously shown for full-length LRRK2 (20).

To determine whether the substitution of the Gly for a Ser residue generated another phosphorylation site within LRRK2, we tested the G2019S mutation on the autophosphorylation-negative T2031A/S2032A mutation. Autophosphorylation assays showed that the triple mutant (G2019S/T2031A/S2032A), but not the double mutant (T2031A/S2032A) incorporated phosphate, indicating that the substituted Ser residue at position 2019 serves as an additional phosphorylation site (Fig. 4C).

To further analyze the mechanism by which the G2019S mutation enhances LRRK2 kinase activity, we mutated this residue to an Ala. The activity of the G2019A mutant was comparable to wild-type (Fig. 4D and E). Thus, the bulkier Ser substitution (and/or its phosphorylation) may selectively enhance catalytic activity by helping to stabilize the N-terminal hinge region of the activation loop, thereby mimicking the active state of the enzyme. To test this possibility, we analyzed residues at the C-terminal hinge region of the activation loop for their effects on catalytic activity. The C-terminal hinge in LRRK2 begins at T2035 (Fig. 3A), a highly conserved residue amongst Ser/Thr protein kinases which seems to play a structural role in maintaining close contact of the activation segment with the catalytic loop (22). The T2035A mutant LRRK2 did not show detectable autophosphorylation (Fig. 4D and E) nor model substrate phosphorylation (data not shown), but was phosphorylated in transphosphorylation reactions (Fig. 3D and E). These results indicate that T2035 is a structural determinant for LRRK2 enzymatic activity, rather than a regulatory phosphorylation site. To determine whether the G2019S mutation would bypass the requirement for T2035, we generated double mutant constructs. The G2019S/T2035A mutant was as hyperactive as G2019S, whereas the G2019A/T2035A mutant was catalytically dead (Fig. 4D and E). Thus, the

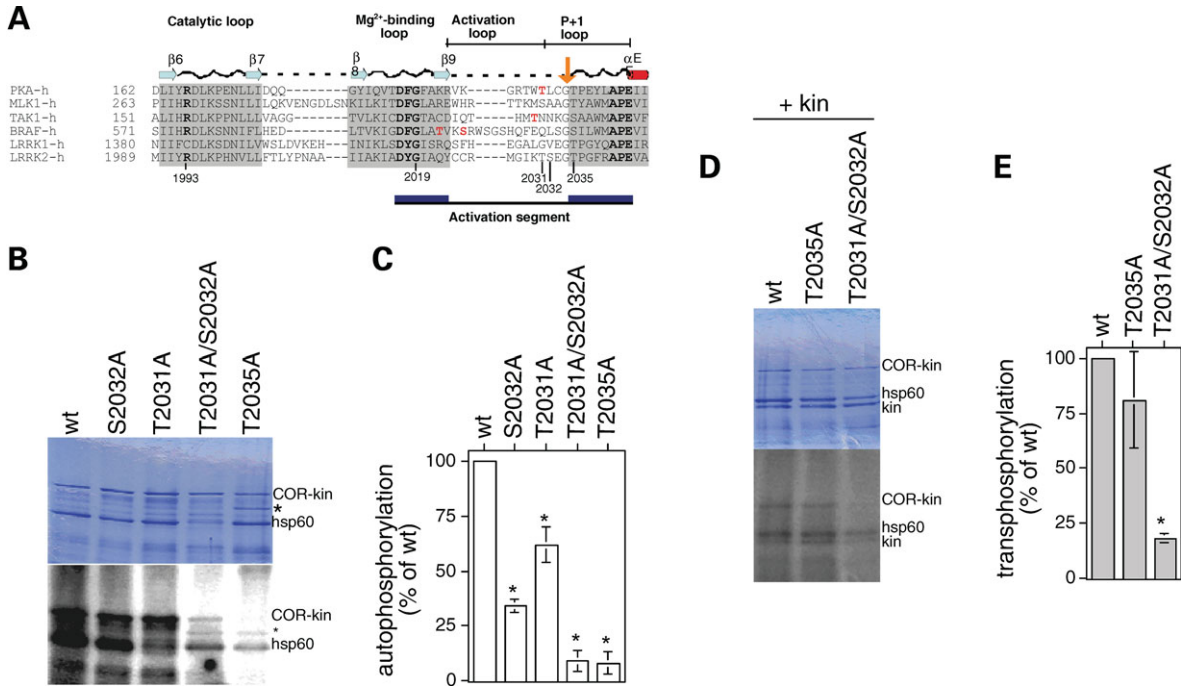

Figure 3. Determination of autophosphorylation sites within recombinant LRRK2 kinase. (**A**) Sequence alignment of the activation segment of LRRK2. The secondary structure of the kinase core of protein kinase A (PKA) is indicated above the alignment (22). Human LRRK2, LRRK1, MLK1, TAK1 and B-Raf were aligned against the sequence of PKA by maximizing alignment across structurally homologous regions of Ser/Thr protein kinases. These structurally conserved regions include the catalytic loop and its flanking β strands (β6 and β7), the Mg^{2+} binding loop and its flanking β strands (β8 and β9), and a segment containing the *P*+1 loop and the ±αEF helix (gray boxes). All kinases regulated through activation segment phosphorylation have a conserved arginine preceding the catalytic aspartate in the catalytic loop (27) (bold). The primary sequence of the activation segment is defined as the region between and including two conserved tripeptide motifs, DF/YG and APE (bold). The N-terminal and C-terminal hinge regions of the activation segment are indicated in blue. For Ser/Thr kinases, the C-terminal hinge region begins at a conserved Ser or Thr residue (orange arrow). The residue immediately preceding the C-terminal hinge region often is a Gly, and its inherent flexibility may be important for kinase activity (22). Phosphorylation sites determined in PKA, TAK1 and B-Raf are indicated in red (35,43,44). The amino acid number of relevant residues in LRRK2 across the sequence alignment is indicated. (**B**) Example of an autophosphorylation experiment using wild-type or the indicated point-mutant COR-kinase proteins. Top: Coomassie; Bottom: ^{32}P autoradiograph. *, contaminant observed in some protein preparations. (**C**) Quantitation of autophosphorylation experiments of the type depicted in (B). Experiments and data analysis were performed as described in legend to Figure 1. The extent of phosphate incorporation was compared to results with wild-type protein and charted as percent of the control measurement. Average values from several experiments (S2032A, $n = 4$; T2031A, $n = 4$; T2031A/S2032A, $n = 3$; T2035A, $n = 6$) are shown. Error bars represent SEM. *, $P < 0.05$. (**D**) Example of a transphosphorylation experiment using wild-type or the T2035A or T2031A/S2032A-point-mutant COR-kinase proteins, together with wild-type kinase domain protein (kin). Top: Coomassie; Bottom: ^{32}P autoradiograph. (**E**) Quantitation of experiments of the type depicted in (D). Experiments and data analysis were performed as described in legend to Figure 1. The extent of phosphate incorporation was compared to results with wild-type protein and charted as percent of the control measurement. Average values from several independent experiments (T2035A, $n = 3$; T2031A/S2032A, $n = 4$) are shown. Error bars represent SEM. *, $P < 0.05$.

pathogenic G2019S mutant seems to reorganize the activation loop in a T2035-independent manner to enhance the catalytic activity of LRRK2. Further, this active-state mimickry is dependent on the bulkier nature (and/or phosphorylation) of the Ser residue, as it was not observed by an equivalent Ala substitution. In this manner, the G2019S mutation seems to modify the structure of the N-terminal hinge of the activation segment to mimick the active state.

DISCUSSION

In the present study, we have examined the effect of select pathogenic mutations on the catalytic activity of purified, recombinant LRRK2 kinase *in vitro*, and the molecular mechanism by which the prominent G2019S mutation may enhance the catalytic activity of LRRK2. Amongst the pathogenic mutations analysed, only the G2019S mutation was found to enhance the kinase activity of LRRK2. Catalytic activity was regulated by intermolecular autophosphorylation on two sites within the activation segment, with the Gly to Ser mutation generating an additional autophosphorylation site. Importantly, wild-type but not G2019S mutant kinase activity was crucially dependent on a residue in the C-terminal hinge region of the activation segment. These data indicate that the G2019S mutation may lead to a conformational change in the activation segment structurally mimicking the active state of the kinase.

The present data describe for the first time conditions suitable for the purification of bacterially expressed, active recombinant LRRK2 kinase. This allows for detailed measurements of the enzymatic activity of recombinant kinase *in vitro*, which should aid in the design of high-throughput drug screening approaches. Indeed, while the activity of many kinases is modulated by separate regulatory domains and/or regulatory proteins (22,28), most inhibitors target the catalytic core of

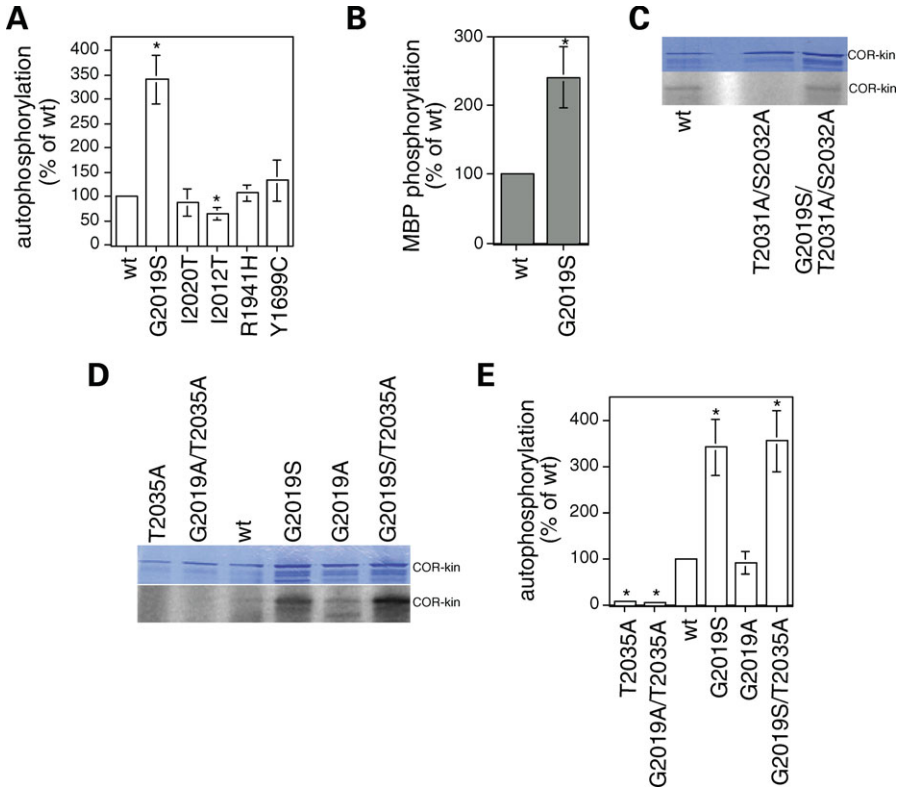

Figure 4. Effect of G2019S mutation on LRRK2 kinase activity. (**A**) Autophosphorylation of wild-type or various mutant COR-kinase proteins. Experiments and data analysis were performed as described in legend to Figure 1. The extent of phosphate incorporation was compared to results with wild-type protein and charted as percent of the control measurement. Average values from several experiments (G2019S, $n = 10$; I2020T, $n = 5$; I2012T, $n = 6$; R1941H, $n = 4$; Y1699C, $n = 5$) are indicated above the individual columns. Error bars represent SEM. *, $P < 0.05$. (**B**) Quantitation of MBP substrate phosphorylation assays with wild-type and G2019S-mutant LRRK2 protein (COR-kinase). Average values from five independent experiments are shown. Error bars represent SEM. *, $P < 0.05$. (**C**) Representative example of autophosphorylation of the phosphorylation-site mutant T2031A/S2032A in the presence or absence of the pathogenic G2019S mutation. Top: Coomassie; Bottom: ^{32}P autoradiograph. (**D**) Example of an autophosphorylation experiment using wild-type or the indicated point-mutant COR-kinase proteins. Top: Coomassie; Bottom: ^{32}P autoradiograph. (**E**) Quantitation of experiments of the type depicted in (D). Experiments and data analysis were performed as described in legend to Figure 1. The extent of phosphate incorporation was compared to results with wild-type protein and charted as percent of the control measurement. Average values from several independent experiments (T2035A; $n = 6$; G2019A/T2035A, $n = 3$; G2019S, $n = 10$; G2019A, $n = 9$; G2019S/T2035A, $n = 3$) are shown. Error bars represent SEM. *, $P < 0.05$.

the kinase (29,30). Therefore, inhibitor screens using the recombinant kinase domain of LRRK2 alone should be sufficient to identify compounds which selectively target LRRK2 kinase.

Recombinant kinase activity was found to be crucially dependent on the presence of Mn^{2+}, while most assays using full-length, immunoprecipitated LRRK2 have been performed in the absence of added Mn^{2+} (20,21,23,24,26). Such discrepancy may be due to traces of endogenous Mn^{2+} bound to immunoprecipitated material. In addition, catalytic activity was found to be profoundly inhibited by negatively charged phospholipids, suggesting that membrane association of LRRK2 (23,26,31,32) may further regulate its kinase activity.

The pathogenic G2019S and I2020T mutations lie within the N-terminal hinge region of the activation segment, which also forms part of the Mg^{2+} binding loop of the kinase. Similarly, the pathogenic I2012T mutation maps to this metal binding loop. Based on such position, mutations in those residues have been hypothesized to abolish the correct positioning of Mg^{2+} within the active site of the kinase, with concomitant decrease in catalytic activity (33). However, a multitude of studies, including ours, indicate that the G2019S mutation leads to enhanced kinase activity, thereby excluding that this mutation abrogates metal binding. On the contrary, our observation that the extent of enhanced catalytic activity of the G2019S mutant versus wild-type LRRK2 kinase is dependent on the concentration of Mn^{2+} (data not shown) may suggest an increase in metal binding capacity, which needs further investigation.

The effect of other pathogenic mutations on LRRK2 kinase activity is more controversial. For example, the I2020T mutation has been documented to either increase (20,26) or decrease (34) the activity of full-length LRRK2, and in our assays had no effect on the kinase activity of recombinant protein. Thus, the mechanism by which this mutation affects LRRK2 function remains unknown. On the other hand, the I2012T mutation was found to decrease the activity of full-length LRRK2 in two independent studies (20,34). Similarly, we found that this mutation decreased the catalytic activity of recombinant kinase. Thus, all currently available data indicate that the I2012T mutation leads to a decrease in LRRK2 kinase activity, and the manner by which this mutation

induces PD thus seems to involve mechanisms unrelated to its kinase activity. Finally, a putatively pathogenic mutation (R1941H) in the kinase domain, as well as a pathogenic mutation in the COR domain (Y1699C) have been described to decrease or increase the activity of full-length LRRK2 kinase, respectively (20,34), but were without effect on the activity of recombinant kinase. Such discrepancy may reflect differences in assay sensitivity or the necessity to examine certain mutations in a full-length context. For example, the COR domain may be responsible for correct positioning of the catalytic Roc and kinase domains with respect to each other, and the effect of mutations in such a domain on catalytic activity may thus only be gauged from studying the full-length protein.

We find that LRRK2 activity is regulated by phosphorylation in the activation segment, as are a large variety of other protein kinases. The kinase-dead LRRK2 mutant (K1906M) was not phosphorylated, indicating that basal activity is required for the regulatory autophosphorylation. Our data show that the catalytic domain of LRRK2 is capable of intermolecular self-phosphorylation and activation in the absence of an upstream activating kinase. This is a feature shared with for example protein kinase A (35), but is distinct from the cascade phosphorylation demonstrated by MAP kinase modules (28). Indeed, recent studies also indicate that full-length LRRK2 expressed in tissue culture cells displays basal kinase activity (36). Thus, while phosphorylation of LRRK2 within regulatory domains by upstream kinases remains a possibility, we speculate that regulation of LRRK2 activity *in vivo* may be controlled by other mechanisms, such as its intrinsic GTP binding and/or GTPase activity (20,21) or its subcellular localization and/or clustering, which would serve to modulate the apparently intrinsic ability of LRRK2 to auto-activate. Phosphorylation-state-specific antibodies against active LRRK2 phosphorylated within the activation segment at the two identified sites will be required in future studies to address such hypothesis.

A conserved Thr residue (T2035) in the C-terminal hinge region of the activation segment seems to be essential for LRRK2 kinase activity, and mutation of the equivalent residue has been shown to affect the activity of other Ser/Thr kinases as well (22,37,38). Our data indicate that this Thr residue may play a crucial role for the rotational movement of the activation loop involved in switching between the active and inactive state of LRRK2. The G2019S mutation in the N-terminal hinge region seems to bypass the requirement for T2035 in the C-terminal hinge, suggesting that the G2019S mutation mimicks the constitutively active conformational status of the activation segment. In addition, this mimickry seems to be dependent on the hydrophilic nature and/or phosphorylation of the serine residue. Such 'active state mimickry' has been reported previously for other kinases implicated in human cancers. For example, some oncogenic mutations in B-RAF or BCR-ABL are situated within the activation segment as well, and have been suggested to destabilize the inactive conformation of the DFG motif/activation segment, mimicking the conformational changes normally promoted by activation segment phosphorylation (39,40). Consideration of such differential conformational states will be important when screening compounds for their ability to inhibit wild-type or G2019S mutant LRRK2 kinase activity (29,30).

The observed intermolecular nature of autophosphorylation and concomitant activation of LRRK2 kinase may explain the absence of a difference in phenotype between heterozygous and homozygous G2019S carriers (41), whereby mutant kinase molecules can phosphorylate wild-type kinase molecules, thereby increasing in a dominant manner the entire cellular and active pool of LRRK2. However, the reported incomplete penetrance (2,12,14–16) suggests that additional mechanism(s) besides regulation of kinase activity *per se* contribute to the pathogenesis of mutant LRRK2. The delineation of LRRK2 function holds great promise for our understanding of the molecular pathways underlying PD.

MATERIALS AND METHODS

Plasmid construction

Constructs encoding sequences for different human LRRK2 domain combinations, Roc-COR-kinase-WD40 (1315–2527), COR-kinase-WD40 (1518–2527), kinase-WD40 (1845–2527), Roc-COR-kinase (1315–2143), COR-kinase (1518–2143) and kinase (1845–2143) were generated by PCR using a human full-length LRRK2 construct and subcloned into the expression plasmid pGEX-KG (42). Domain boundaries were established based on BLASTP sequence alignments and the previously described domain architecture of Roco proteins (19). The kinase and Roc-COR-kinase constructs were subcloned via the XbaI/XhoI restriction sites, whereas the other constructs were subcloned non-directionally via the XbaI restriction site. The glycine linker encoded in the pGEX-KG plasmid, which separates the GST moiety and the thrombin cleavage site from the different LRRK2 fusion domains, was found to be crucial for efficient purification of active LRRK2 protein. The entire coding sequences of all constructs were verified by DNA sequencing.

Mutant constructs were generated using the QuickChange mutagenesis kit (Stratagene) according to manufacturer's instructions and resequenced as indicated above. The sequences of all primers used in the present study are available upon author's request.

Protein purification

All recombinant proteins were expressed as N-terminally tagged GST fusion proteins in *E.coli* BL21 cells. Due to the limited solubility of the larger recombinant proteins, only COR-kinase and kinase domain proteins were analyzed in the present study. For this purpose, an overnight culture of cells was diluted 10-fold and grown at 16°C to an OD_{600} of around 0.6, followed by induction with 0.1 mM IPTG at 16°C overnight. Cells were pelleted at 10 000*g* for 12 min, and the pellet was resuspended in 6 ml (per liter culture) of resuspension buffer [PBS containing 1% Triton-X100, 100 μM phenylmethylsulfonyl fluoride (PMSF), 1 mM DTT, 50 μg/ml RNase, 5 μg/ml DNase and 100 μg/ml lysozyme]. The cell resuspension was incubated for 30 min at 4°C on a rotary shaker, followed by four sonication pulses (30 s each, separated by 15 s intervals) on ice. Note that the gentle

(albeit inefficient) disruption of cells by short sonication pulses yielded less, but significantly more active recombinant LRRK2 protein than that obtained by the use of a French Press. Upon centrifugation at 16 000*g* for 30 min at 4°C, the soluble fraction was filtered through a 0.22 μm filter and diluted with an equal volume of resuspension buffer. Proteins were bound to glutathione Sepharose beads (Pharmacia) (500 μl of packed bead volume per liter culture) for 2 h at 4°C in binding buffer (PBS containing 1% Triton-X100, 100 μM PMSF and 1 mM DTT), followed by 12 washes in binding buffer and 6 washes in elution buffer (50 mM Tris–HCl pH 8.0, 1% Triton-X100, 100 μM PMSF and 1 mM DTT). Proteins were eluted with 20 mM glutathione in elution buffer (six times 500 μl for 15 min at 4°C on rotary shaker). Note that neither the presence of Triton-X100 (as compared to proteins purified in the absence of detergent) nor the GST moiety (as compared to proteins eluted by the addition of thrombin) adversely affected LRRK2 kinase activity. Protein concentrations were estimated using the Bradford (Bio-Rad) assay with bovine serum albumin as a standard. Small aliquots of recombinant LRRK2 proteins were flash-frozen in liquid N_2, stored at −80°C and only thawed up once.

Phosphorylation reactions

Unless otherwise indicated, the buffer used for phosphorylation reactions contained 50 mM HEPES pH 7.4, 5 mM $MgCl_2$, 5 mM $MnCl_2$ and 0.5 mM DTT. LRRK2 recombinant protein (1 μg) was preincubated in phosphorylation buffer for 1 min at 24°C, and reactions were initiated by the addition of [γ- ^{32}P]ATP (final concentration, 100 μM). Reactions were carried out in a final volume of 40 μl. After 30 min at 24°C, reactions were terminated by the addition of 0.2 volumes of 5× sample buffer and heating for 5 min at 95°C. Transphosphorylation reactions contained 0.5 μg of COR-kinase and 2 μg of kinase proteins. Substrate phosphorylation assays contained 10 μg MBP.

Proteins were separated by SDS–PAGE on 7.5% polyacrylamide gels (or 12.5% gels for assays containing MBP), followed by staining with Coomassie blue dye. Incorporation of ^{32}P was quantitated by using a PhosphorImager (Molecular Dynamics). Radioactive bands were quantified using ImageQuant (Molecular Dynamics), and corrected for background values. Differences in protein amounts were quantified on Coomassie stained gels using QuantityOne (Bio-Rad), and corrected for background values, and radioactivity values were corrected for differences in protein loading. Experiments were done the indicated amount of times, and the data were analyzed using the paired Student's *t*-test.

Materials

Phosphatidylserine was from Avanti Polar Lipids. [γ-^{32}P]ATP (specific activity, 150mCi/ml) was from *GE*Healthcare. MBP was a gift from Prof. Paul Greengard. All other chemicals were of reagent grade or better.

ACKNOWLEDGEMENTS

We thank Angus Nairn and Ignacio Mata for critical reading of an early version of the manuscript. This work is supported by grants from the Parkinson's Disease Foundation, the Fundación Ramón Areces and the Spanish Health Ministry (FIS). S.H. is supported by a Ramón y Cajal Fellowship.

Conflict of Interest Statment. The authors declare no conflicts of interest.

REFERENCES

1. Paisan-Ruiz, C., Jain, S., Evans, E.W., Gilks, W.P., Simon, J., van der Brug, M., Lopez de Munain, A., Aparicio, S., Gil, A.M., Khan, N. *et al.* (2004) Cloning of the gene containing mutations that cause PARK8-linked Parkinson's disease. *Neuron*, **44**, 595–600.
2. Zimprich, A., Biskup, S., Leitner, P., Lichtner, P., Farrer, M., Lincoln, S., Kachergus, J., Hulihan, M., Uitti, R.J., Calne, D.B. *et al.* (2004) Mutations in LRRK2 cause autosomal-dominant parkinsonism with pleomorphic pathology. *Neuron*, **44**, 601–607.
3. Di Fonzo, A., Rohe, C.F., Ferreira, J., Chien, H.F., Vacca, L., Stocchi, F., Guedes, L., Fabrizio, E., Manfredi, M., Vanacore, N. *et al.* (2005) A frequent LRRK2 gene mutation associated with autosomal dominant Parkinson's disease. *Lancet*, **365**, 412–415.
4. Gilks, W.P., Abou-Sleiman, P.M., Gandhi, S., Jain, S., Singleton, A., Lees, A.J., Shaw, K., Bhatia, K.P., Bonifati, V., Quinn, N.P. *et al.* (2005) A common LRRK2 mutation in idiopathic Parkinson's disease. *Lancet*, **365**, 415–416.
5. Clark, L.N., Wang, Y., Karlins, E., Saito, L., Mejia-Santana, H., Harris, J., Louis, E.D., Cote, L.J., Andrews, H., Fahn, S. *et al.* (2006) Frequency of LRRK2 mutations in early- and late-onset Parkinson disease. *Neurology*, **67**, 1786–1791.
6. Gaig, C., Ezquerra, M., Marti, M.J., Munoz, E., Valldeoriola, F. and Tolosa, E. (2006) LRRK2 mutations in Spanish patients with Parkinson disease: frequency, clinical features, and incomplete penetrance. *Arch. Neurol.*, **63**, 377–382.
7. Ishihara, L., Gibson, R.A., Warren, L., Amouri, R., Lyons, K., Wielinski, C., Hunter, C., Swartz, J.E., Elango, R., Akkari, P.A. *et al.* (2007) Screening for Lrrk2 G2019S and clinical comparison of Tunisian and North American Caucasian Parkinson's disease. *Mov. Disord.*, **22**, 55–61.
8. Lesage, S., Durr, A., Tazir, M., Lohmann, E., Leutenegger, A.L., Janin, S., Pollak, P. and Brice, A. (2006) LRRK2 G2019S as a cause of Parkinson's disease in North African Arabs. *N. Engl. J. Med.*, **354**, 422–423.
9. Ozelius, L.J., Senthil, G., Saunders-Pullman, R., Ohmann, E., Deligtisch, A., Tagliati, M., Hunt, A.L., Klein, C., Henick, B., Hailpern, S.M. *et al.* (2006) LRRK2 G2019S as a cause of Parkinson's disease in Ashkenazi Jews. *N. Engl. J. Med.*, **354**, 424–425.
10. Tan, E.K., Shen, H., Tan, L.C., Farrer, M., Yew, K., Chua, E., Jamora, R.D., Puvan, K., Puong, K.Y., Zhao, Y. *et al.* (2005) The G2019S LRRK2 mutation is uncommon in an Asian cohort of Parkinson's disease patients. *Neurosci. Lett.*, **384**, 327–329.
11. Lu, C.S., Simons, E.J., Wu-Chou, Y.H., Fonzo, A.D., Chang, H.C., Chen, R.S., Weng, Y.H., Rohe, C.F., Breedveld, G.J., Hattori, N. *et al.* (2005) The LRRK2 I2012T, G2019S and I2020T mutations are rare in Taiwanese patients with sporadic Parkinson's disease. *Parkinsonism Relat. Disord.*, **11**, 521–522.
12. Kachergus, J., Mata, I.F., Hulihan, M., Taylor, J.P., Lincoln, S., Aasly, J., Gibson, J.M., Ross, O.A., Lynch, T., Wiley, J. *et al.* (2005) Identification of a novel LRRK2 mutation linked to autosomal dominant parkinsonism: evidence of a common founder across European populations. *Am. J. Hum. Genet.*, **76**, 672–680.
13. Zabetian, C.P., Hutter, C.M., Yearout, D., Lopez, A.N., Factor, S.A., Griffith, A., Leis, B.C., Bird, T.D., Nutt, J.G., Higgins, D.S. *et al.* (2006) LRRK2 G2019S in families with Parkinson disease who originated from Europe and the Middle East: evidence of two distinct founding events beginning two millenia ago. *Am. J. Hum. Genet.*, **79**, 752–758.
14. Zabetian, C.P., Samii, A., Mosley, A.D., Roberts, J.W., Leis, B.C., Yearout, D., Raskind, W.H. and Griffith, A. (2005) A clinic-based study of the LRRK2 gene in Parkinson disease yields new mutations. *Neurology*, **65**, 741–744.

15. Kay, D.M., Kramer, P., Higgins, D., Zabetian, C.P. and Payami, H. (2005) Escaping Parkinson's disease: a neurologically healthy octogenarian with the LRRK2 G2019S mutation. *Mov. Disord.*, **20**, 1077–1078.
16. Tan, E.K., Skipper, L., Chua, E., Wong, M.C., Pavanni, R., Bonnard, C., Kolatkar, P. and Liu, J.J. (2006) Analysis of 14 LRRK2 mutations in Parkinson's plus syndromes and late-onset Parkinson's disease. *Mov. Disord.*, **21**, 997–1001.
17. Mata, I.F., Wedemeyer, W.J., Farrer, M.J., Taylor, J.P. and Gallo, K.A. (2006) LRRK2 in Parkinson's disease: protein domains and functional insights. *Trends Neurosci.*, **29**, 286–293.
18. Marin, I. (2006) The Parkinson Disease gene LRRK2: evolutionary and structural insights. *Mol. Biol. Evol.*, **23**, 2423–2433.
19. Bosgraaf, L. and Van Haastert, P.J. (2003) Roc, a Ras/GTPase domain in complex proteins. *Biochim. Biophys. Acta*, **1643**, 5–10.
20. West, A.B., Moore, D.J., Choi, C., Andrabi, S.A., Li, X., Dikeman, D., Biskup, S., Zhang, Z., Lim, K.-L., Dawson, V.L. *et al.* (2007) Parkinson's disease-associated mutations in LRRK2 link enhanced GTP-binding and kinase activities to neuronal toxicity. *Hum. Mol. Genet.*, **16**, 223–232.
21. Ito, G., Okai, T., Fujino, G., Takeda, K., Ichijo, H., Katada, T. and Iwatsubo, T. (2007) GTP binding is essential to the protein kinase activity of LRRK2, a causative gene product for familial Parkinson's disease. *Biochemistry*, **46**, 1380–1388.
22. Nolen, B., Taylor, S. and Ghosh, G. (2004) Regulation of protein kinases: controlling activity through activation segment conformation. *Mol. Cell*, **15**, 661–675.
23. West, A.B., Moore, D.J., Biskup, S., Bugayenko, A., Smith, W.W., Ross, C.A., Dawson, V.L. and Dawson, T.M. (2005) Parkinson's disease-associated mutations in leucine-rich repeat kinase 2 augment kinase activity. *Proc. Natl Acad. Sci. USA*, **102**, 16842–16847.
24. Smith, W.W., Pei, Z., Jiang, H., Dawson, V.L., Dawson, T.M. and Ross, C.A. (2006) Kinase activity of mutant LRRK2 mediates neuronal toxicity. *Nat. Neurosci.*, **9**, 1231–1233.
25. Greggio, E., Jain, S., Kingsbury, A., Bandopadhyay, R., Lewis, P., Kaganovich, A., van der Brug, M.P., Beilina, A., Blackinton, J., Thomas, K.J. *et al.* (2006) Kinase activity is required for the toxic effects of mutant LRRK2/dardarin. *Neurobiol. Dis.*, **23**, 329–341.
26. Gloeckner, C.J., Kinkl, N., Schumacher, A., Braun, R.J., O'Neill, E., Meitinger, T., Kolch, W., Prokisch, H. and Ueffing, M. (2006) The Parkinson disease causing LRRK2 mutation I2020T is associated with increased kinase activity. *Hum. Mol. Genet.*, **15**, 223–232.
27. Johnson, L.N., Noble, M.E.M. and Owen, D.J. (1996) Active and inactive protein kinases: structural basis for regulation. *Cell*, **85**, 149–158.
28. Huse, M. and Kuriyan, J. (2002) The conformational plasticity of protein kinases. *Cell*, **109**, 275–282.
29. Knight, Z.A. and Shokat, K.M. (2005) Features of selective kinase inhibitors. *Chem. Biol.*, **12**, 621–637.
30. Noble, M.E.M., Endicott, J.A. and Johnson, L.N. (2004) Protein kinase inhibitors: insights into drug design from structure. *Science*, **303**, 1800–1805.
31. Biskup, S., Moore, D.J., Celsi, F., Higashi, S., West, A.B., Andrabi, S.A., Kurkinen, K., Yu, S.W., Savitt, J.M., Waldvogel, H.J. *et al.* (2006) Localization of LRRK2 to membranous and vesicular structures in mammalian brain. *Ann. Neurol.*, **60**, 557–569.
32. Hatano, T., Kubo, S., Imai, S., Maeda, M., Ishikawa, K., Mizuno, Y. and Hattori, N. (2007) Leucine-rich repeat kinase 2 associates with lipid rafts. *Hum. Mol. Genet.*, **16**, 678–690.
33. Albrecht, M. (2005) LRRK2 mutations and Parkinsonism. *Lancet*, **365**, 1230.
34. Jaleel, M., Nichols, R.J., Deak, M., Campbell, D.G., Gillardon, F., Knebel, A. and Alessi, D.R. (2007) LRRK2 phosphorylates moesin at Thr558; characterisation of how Parkinson's disease mutants affect kinase activity. *Biochem. J.*, doi: 10.1042/BJ20070209.
35. Knighton, D.R., Zheng, J.H., Ten Eyck, L.F., Ashford, V.A., Wuong, N.H., Taylor, S.S. and Sowadski, J.M. (1991) Crystal structure of the catalytic subunit of cyclic adenosine monophosphate-dependent protein kinase. *Science*, **253**, 407–414.
36. Greggio, E., Lewis, P.A., van der Brug, M.P., Ahmad, R., Kaganovich, A., Ding, J., Beilina, A., Baker, A.K. and Cookson, M.R. (2007) Mutations in LRRK2/dardarin associated with Parkinson disease are more toxic than equivalent mutations in the homologous kinase LRRK1. *J. Neurochem.*, **102**, 93–102.
37. Szczepanowska, J., Ramachandran, U., Herring, C.J., Gruschus, J.M., Qin, J., Korn, E. and Brzeska, H. (1998) Effect of mutating the regulatory phosphoserine and conserved threonine on the activity of the expressed catalytic domain of *Acanthamoeba* myosin I heavy chain kinase. *Proc. Natl Acad. Sci. USA*, **95**, 4146–4151.
38. Moore, M.J., Kanter, J.R., Jones, K.C. and Taylor, S.S. (2002) Phosphorylation of the catalytic subunit of protein kinase A. *J. Biol. Chem.*, **277**, 47878–47884.
39. Wan, P.T., Garnett, M.J., Roe, S.M., Lee, S., Niculescu-Duvaz, D., Good, V.M., Jones, C.M., Marshall, C.J., Springer, C.J., Barford, D. and Marais, R. Cancer Genome Project (2004) Mechanism of activation of the RAF-ERK signaling pathway by oncogenic mutations of B-RAF. *Cell*, **116**, 855–867.
40. Azam, M., Latek, R.R. and Daley, G.Q. (2003) Mechanisms of autoinhibition and STI-571/imatinib resistance revealed by mutagenesis of BCR-ABL. *Cell*, **112**, 831–843.
41. Ishihara, L., Warren, L., Gibson, R., Amouri, R., Lasage, S., Durr, A., Tazir, M., Wszolek, Z.K., Uitti, R.J., Nichols, W.C. *et al.* (2006) Clinical features of Parkinson disease patients with homozygous leucine-rich repeat kinase 2 G2019S mutations. *Arch. Neurol.*, **63**, 1250–1254.
42. Guan, K.L. and Dixon, J.E. (1991) Eukaryotic proteins expressed in *Escherichia coli*: an improved thrombin cleavage and purification procedure of fusion proteins with glutathione S-transferase. *Anal. Biochem.*, **192**, 262–267.
43. Zhang, B.H. and Guan, K.L. (2000) Activation of B-raf kinase requires phosphorylation of the conserved residues Thr598 and Ser601. *EMBO J.*, **19**, 5429–5439.
44. Singhirunnusorn, P., Suzuki, S., Kawasaki, N., Saiki, I. and Sakurai, H. (2005) Critical roles of threonine 187 phosphorylation in cellular stress-induced rapid and transient activation of transforming growth factor-β-activated kinase 1 (TAK1) in a signaling complex containing TAK1-binding protein TAB1 and TAB2. *J. Biol. Chem.*, **280**, 7359–7368.